BP compound exhibits imaginary frequencies for the lowest energy vibration in the nondegenerate A″ and doubly degenerate E″ modes. The eigenvectors for these two modes are out-of-plane puckering motions. Also reported in Table VII are the frequencies for the BP compound obtained when the dihedral angles maintaining the ring's planarity were permitted to relax, a new optimum obtained, and the resulting nonplanar geometry shown in Figure 2 was used in a frequency calculation. This nonplanar optimum can be described as a puckered ring with an elongated middle between the two three-atom ends. One end is a PHBHPH piece while the other is a BHPHBH piece. The BP distance between the pieces is 1.935 Å, while the BP distances within both end pieces is 1.866 Å. The PH distances increased somewhat compared with the planar constrained form to 1.392 Å, but the BH distances are essentially unchanged at 1.185 Å. The calculated frequencies are all real for this structure, demonstrating that it is a true minimum, but we have made no effort to establish that it is the absolute minimum. The preference of the BP compound for the puckered ring is closely related to the preference of PH_2BH_2 to pyramidalize at phosphorus as reported by Allen, Scheiner, and Schaefer.[34] For the puckered ring, the out-of-plane angle at each of the phosphorus atoms is about 60°, while that at boron is ten times smaller or about 6°. Allen, Scheiner, and Schaefer[34] report 70 and 6° respectively for the out-of-plane angles in PH_2BH_2.

Conclusion

Ab initio electronic structure calculations systematically investigating a hierarchy of basis sets and including correlation effects via perturbation theory have been applied to assist in understanding the chemistry of the recently synthesized heteropolar III–V analogues of benzene. The rich literature investigating aromaticity in organic molecules led us to rely most heavily upon the use of homodesmotic reaction sequences to establish an aromatic index for these compounds. An isodesmic hydrogen transfer reaction corroborates the relative trend of aromaticity, but would differ in its attribution of antiaromaticity to all of the heteropolar compounds. The attribution of antiaromaticity to compounds whose experimental behavior is aromatic has been a common deficiency in many reaction sequences suggested for indices of aromaticity, but the homodesmotic scheme appears to be more satisfactory in this regard. The relative aromaticity established by the homodesmotic reaction energy for the six-membered-ring analogues of benzene is CC ≫ BP ~ BN > AlN. The BP compound is calculated to prefer a nonplanar geometry pyramidal at phosphorus as has been previously reported for the ethylene analogue BH_2PH_2. The bulky substituents on the ring of the synthesized BP compounds may be playing a role in keeping the planar geometry.

Acknowledgment. We would like to acknowledge stimulating discussions with Philip Power and Krista Waggoner throughout the course of this work. The work was performed largely on the Data General MV/10000 computer which was purchased with the aid of NSF Grant CHE 8420185. Additional computing resource was made available at the San Diego Supercomputer Center and The Office of Academic Computing at UCLA. We would also like to acknowledge Wesley Allen for conversations about homodesmotic reactions and Ed Motell for enabling a calculation on the CSU Multiflow Trace facility.

(34) Allen, Thomas L.; Scheiner, Andrew C.; Schaefer, Henry F. III *Inorg. Chem.* **1990**, *29*, 1930–1936.

New Synthetic Approach to Extended Solids: Selective Synthesis of Iron Silicides via the Amorphous State

Thomas Novet and David C. Johnson*

Contribution from the Department of Chemistry, University of Oregon, Eugene, Oregon 97403.
Received September 10, 1990

Abstract: A new synthetic approach in which thin (15–50 Å) amorphous elemental layers are sequentially deposited to create a unique initial reactant is described. This new approach overcomes the limitations of traditional, diffusion-limited, solid-state synthetic methods, which offer no control of the reaction pathway and therefore no control over which intermediates are formed. In our synthetic approach, the initial layered composite is diffused at low temperatures to produce a homogeneous amorphous alloy; nucleation is then the rate-limiting step in the formation of a crystalline material. The layered nature of the starting reactant permits the reaction to be followed in a quantitative manner with use of X-ray diffraction. The composition-directed crystallization of iron silicides from homogeneous amorphous alloy intermediates is described as a first example of our new synthetic method. The resultant iron silicides all crystallized below 550 °C, including Fe_5Si_3, which is metastable with respect to a mixture of FeSi and $FeSi_3$ below 825 °C.

Introduction

Many of the basic principles and concepts used by molecular chemists only apply to a small fraction of solid-state compounds. An example of one of these principles is the law of definite proportions, the concept that a compound has a definite stoichiometry. Nonstoichiometric extended solids such as FeO_x with $1.05 < x < 1.13$ are common to many solid-state phase diagrams. Another example is the ability of molecular chemists to predict the structure and reactivity of an unknown compound based on a knowledge of the bonding and coordination of the atoms involved. Except for simple derivative compounds based upon simple chemical substitution, the ability to predict the structures of new solid-state compounds is practically impossible due to the large variability in coordination numbers found in extended solids. The concept of a reaction mechanism is another well-developed principle of molecular chemistry. Its usefulness in solid-state synthesis has been limited, since most solid-state synthetic techniques produce thermodynamic products. Also, most solid-state synthesis techniques do not permit the course of a reaction to be followed. It is the concept of a reaction mechanism that we will expand in this paper and apply to the synthesis of extended solids.

The synthetic strategies involved in the preparation of molecular compounds are directed at controlling the kinetics of chemical reactions. Chemists adjust experimental conditions so as to optimize the fraction of starting material that reacts along the desired kinetic pathway. In contrast, the synthetic strategies directed at

0002-7863/91/1513-3398$02.50/0

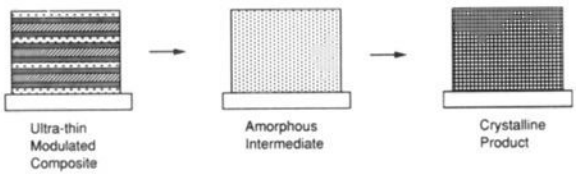

Figure 1. Schematic presentation of the synthetic approach presented in this paper.

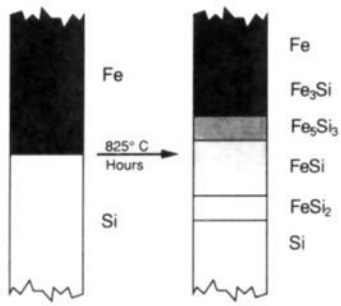

Figure 2. Schematic presentation of an iron–silicon diffusion couple heated at 825 °C for several hours.

extended solids are limited by the high activation energies for diffusion and the long diffusion times in solids. The intermediates involved in these reactions are themselves stable crystalline materials, which limits the range of products that can form. This paper presents a new approach to the kinetically controlled synthesis of extended solids in which nucleation of a crystalline solid is the rate-limiting step. This is illustrated in Figure 1. The key synthetic intermediate is an amorphous alloy formed from the low-temperature diffusion of an ultrathin layered composite.

The direct solid-state reaction between two elements is limited by interdiffusion of the elements. High temperatures and long reaction times are usually necessary for extensive reactions between bulk elements as a result of the high activation energies of diffusion in the solid state.[1] In this diffusion-limited regime, selectivity is nonexistent since every thermodynamically stable binary phase in the phase diagram will nucleate.[2] Hence, the relative amounts of the various compounds will be determined by the diffusion constants of the elements through each of the compounds formed (Figure 2). As a result of this behavior, bulk diffusion couples have long been used to probe phase diagrams and to determine the existence of stable binary phases.[2] Thus, conventional approaches to the synthesis of ternary compounds involve stable binary compounds as intermediates, limiting products to those more thermodynamically stable than the binary compounds in the relevant phase diagrams.

In the 1970s and early 1980s, several research groups began to explore the reaction kinetics of thin-film diffusion couples.[3-12] These groups focused their studies on metal–silicon systems, which are important in the fabrication of integrated circuits. Crystalline films of approximately 500 Å of each element were deposited and subsequently annealed at temperatures of several hundred degrees Celsius to interdiffuse the elements. These thin-film diffusion couples were found to be nucleation-limited rather than diffusion-limited systems. A sequential evolution of the various compounds in the phase diagram was observed, and not all of the compounds in the phase diagram were necessarily formed. The same sequence of phases was observed regardless of the overall composition of the diffusion couple.[13] Figure 3 illustrates the behavior observed for the iron–silicon thin-film diffusion couple, in which Fe_5Si_3 does not nucleate.[14]

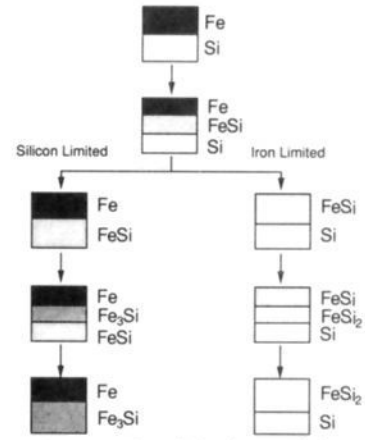

Figure 3. Schematic presentation of the phase evolution of an iron–silicon thin-film diffusion couple.

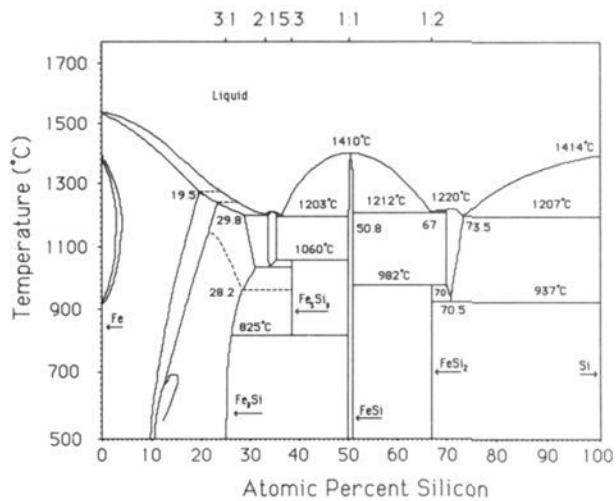

Figure 4. Iron–silicon phase diagram. Reprinted from ref 16. Copyright 1986 ASM International. The iron to silicon ratios of samples prepared in this study are indicated on the upper horizontal axis.

Walser and Bene[15] provided another historically important development. They compiled available data on the binary silicides and empirically correlated the first phase formed in a thin-film diffusion couple with information contained in bulk equilibrium phase diagrams. Their "First Phase Rule" states "The first compound nucleated in planar binary reaction couples is the most stable congruently melting compound adjacent to the lowest temperature eutectic on the bulk equilibrium phase diagram."[15] This empirical rule is remarkably successful at predicting the first phase formed in thin-film diffusion couples, successfully predicting the first phase in 13 out of 14 transition metal–silicon systems studied. To illustrate its application to the iron–silicon system, Figure 4 contains the equilibrium Fe–Si phase diagram.[16] The

(1) Brewer, L. *J. Chem. Educ.* **1958**, *35*, 153.
(2) Brophy, J. H.; Rose, R. M.; Wulff, J. *The Structure and Properties of Materials*; John Wiley and Sons: New York, 1964; Vol. 2, pp 91–94.
(3) Herd, S.; Tu, K. N.; Ahn, K. Y. *Appl. Phys. Lett.* **1983**, *42*, 597.
(4) Nava, F.; Psaras, P. A.; Takai, H.; Tu, K. N. *J. Appl. Phys.* **1986**, *59*, 2429.
(5) Gas, P.; Tardy, F. J.; D'Heurle, F. M. *J. Appl. Phys.* **1986**, *60*, 193.
(6) Gas, P.; D'Heurle, F. M.; Goues, F. K.; La Placa, S. J. *J. Appl. Phys.* **1986**, *59*, 3458.
(7) Coulman, B.; Chen, H. *J. Appl. Phys.* **1986**, *59*, 3467.
(8) Majni, G.; Costato, M.; Panini, F. *Thin Solid Films* **1985**, *125*, 71.
(9) Rosenblum, M. P.; Turnbull, D. *J. Non-Cryst. Solids* **1980**, *37*, 45.
(10) Canali, C.; Majni, G.; Ottaviani, G.; Celotti, G. *J. Appl. Phys.* **1979**, *50*, 255–258.
(11) Canali, C.; Cetellani, F.; Ottaviani, G.; Prudenza, M. *Appl. Phys. Lett.* **1978**, *33*, 187–190.
(12) Ziegler, J. F.; Mayer, J. W.; Kircher, C. J. *J. Appl. Phys.* **1973**, *44*, 3851–3857.
(13) Tsaur, B. Y.; Lau, S. S.; Mayer, J. W.; Nicolet, M. A. *Appl. Phys. Lett.* **1981**, *33*, 922–924.
(14) Lau, S. S.; Feng, J. S. Y.; Olowolafe, J. O.; Nicolet, M. A. *Thin Solid Films* **1975**, *25*, 415.
(15) Walser, R. M.; Bene, R. W. *Appl. Phys. Lett.* **1976**, *28*, 624–625.
(16) Massalski, T. B.; Bennet, L. H., Murray, J. L., Baker, H., Eds. *Binary Alloy Phase Diagrams*; ASM Internationaal: Metals Park, OH, 1990; Vol. 2, p 1772.

lowest melting eutectic is located at 34 atomic percent silicon, and the congruently melting compound with the highest melting point adjacent to this eutectic is FeSi. FeSi is the first phase nucleated in a thin-film diffusion couple as shown in Figure 3.

Walser and Bene speculated on the physical basis for their rule. It was known that an amorphous region develops at the interface between two solid reactants.[17] Walser and Bene reasoned that the composition of this amorphous intermediate would be close to that of the deepest eutectic, since the deepest eutectic represented the most stable liquid in the phase diagram. From this amorphous region, the most likely phase to nucleate would be the one with the largest free energy gain.[15]

We reasoned that if one prepared homogeneous amorphous alloys of varying composition, the phase nucleated from these alloys would then depend on the free energy gain per unit volume of the various potential compounds. We also reasoned, however, that an additional energy term affecting the formation of a crystalline phase is the barrier to nucleation, a kinetic factor not found in an equilibrium phase diagram. The nucleation barrier depends upon the free energy gain per unit volume,[18] surface energy of the growing embryo,[18] internal stress in the film,[18] and the energy necessary to rearrange the amorphous alloy.[18] This last term is minimized for the crystalline phase closest to the composition of the amorphous alloy. If the rearrangement energy is large relative to the other terms, *composition could control the crystalline phase that nucleates.*

In the middle 1980s, several research groups observed that multilayer composites consisting of crystalline elemental metal layers approximately 500 Å thick interdiffused at low temperatures to form homogeneous amorphous alloys.[19-29] Subsequent work demonstrated that both an anomalously large diffusion rate of one metal into the other and a large entropy of mixing are important in this reaction.[22,30-33] It was also found that the thickness of the individual layers in the film must be maintained below an upper limit if the film is to become completely amorphous. In films that exceed this limit, the crystalline alloy nucleates before interdiffusion is complete. It was proposed that the time- and temperature-dependent processes of interdiffusion and nucleation compete in this reaction.[21]

On the basis of this previous work, we hypothesized that *amorphous alloys of almost any composition could be prepared if the initial layer thicknesses were thin enough.* We chose to use layered composites rather than amorphous alloys as our starting point because quantitative information about the diffusion process may be obtained by following the diffusion of the multilayer via X-ray diffraction. This information may then be used to tailor the structure of the initial layered reactant to control its reaction pathway. This paper reports the successful preparation of amorphous composites spanning the iron–silicon phase diagram. Crystallization studies done on these amorphous alloys demonstrated the strong influence of composition upon nucleation. We observe the formation of the binary iron silicides corresponding to the composition of the amorphous alloys, including Fe_5Si_3, which is metastable at the temperature at which it nucleated.

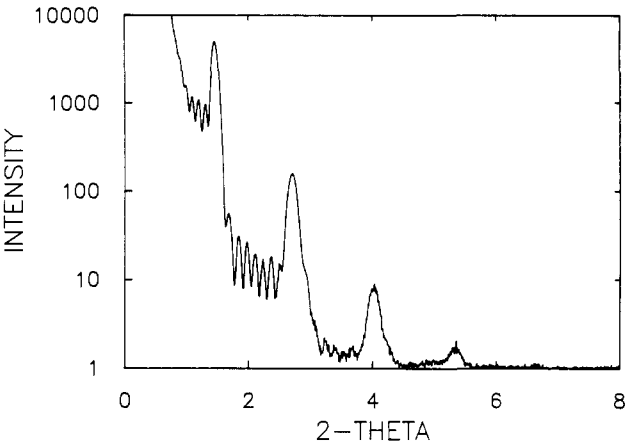

Figure 5. Grazing-angle diffraction pattern of a 10-layer Fe_3Si sample with a multilayer spacing of 66 Å.

These results suggest that it should be possible to prepare ternary compounds directly from amorphous intermediates, avoiding binary compounds as stable, reaction-ending intermediates. The ability to tailor the structure of the layered starting reactant and follow the course of the reaction via in situ techniques should also permit the reaction intermediates to be varied by changing the structure of the layered starting reactant.

Experimental Section

Synthesis of Modulated Composites. The amorphous modulated multilayer composites are prepared in a unique ultrahigh-vacuum deposition system, which is described in detail elsewhere.[34] This system permits the layer thicknesses, the relative position of the elements, and the relative composition of the sample to be controlled. Both iron and silicon were deposited with use of electron-beam guns controlled via quartz crystal thickness monitors. Deposition rates of 0.5 Å/s were used and the background pressure of the chamber during deposition was 5×10^{-8} Torr. A set of samples was synthesized corresponding to the composition of each known compound in the Fe–Si phase diagram ($FeSi_2$, FeSi, Fe_5Si_3, Fe_3Si) and a eutectic composition (34 atomic percent iron). The thickness of the various layers was chosen to achieve the desired stoichiometry and to obtain a repeat until thickness of 60 ± 1 Å. The number of repeat units deposited in each sample varied from 40 to 87 except for one sample of composition 3/1 iron/silicon, which had only ten repeat units.

Grazing- and High-Angle X-ray Diffraction. Both grazing- and high-angle X-ray diffraction data were collected on a Scintag XDS 2000 θ–θ diffractometer for the Fe–Si multilayers presented in this paper. It was necessary to replace the commercial sample stage with a sample mount containing optical flats against which the sample is held with spring tension. The vertical position of the sample stage can be varied with use of a vertical position stage with 0.0001-in. micrometer movement. This movement is necessary to align the sample stage for the grazing-angle studies. The alignment of the sample stage was confirmed before each diffraction session by reproducing a diffraction pattern from a standard layered sample. The high-temperature diffraction data was collected via a high-temperature attachment, which is described in detail elsewhere.[35]

Differential Scanning Calorimetry (DSC). Heat produced by the interdiffusion and crystallization of the Fe–Si multilayers was quantified by DSC. Approximately 1 mg of sample free of the substrate was used. These samples were obtained by first coating a 3-in. silicon wafer with approximately 4000 Å of poly(methyl methacrylate) (PMMA) with use of a 3% solution in chlorobenzene deposited by spin coating at 1000 rpm. The desired multilayer structure was then deposited upon the PMMA-coated substrate. To obtain 1 mg of an Fe–Si multilayer sample, approximately 40 layers with a thickness of 60 Å/layer must be deposited upon a 20 cm^2 area. After the sample was removed from the chamber, it was immersed in acetone, which dissolves the PMMA, floating the

(17) Duwez, P. *Trans. Am. Soc. Met.* **1967**, *60*, 607.
(18) Brophy, J. H.; Rose, R. M.; Wulff, J. *The Structure and Properties of Materials*; John Wiley and Sons: New York, 1964; Vol. 2, pp 98–108.
(19) Van Rossum, M.; Nicolet, M. A.; Johnson, W. L. *Phys. Rev.* **1984**, *B29* 5498.
(20) Clemens, B. M. *Phys. Rev.* **1986**, *B33*, 7615.
(21) Clemens, B. M.; Johnson, W. L.; Schwarz, R. B. *J. Non-Cryst. Solids* **1984**, *61*, *62*, 817.
(22) Schwarz, R. B.; Johnson, W. L. *Phys. Rev. Lett.* **1983**, *51*, 415–418.
(23) Schroder, H.; Samwer, K.; Koster, U. *Phys. Rev. Lett.* **1985**, *54*, 197.
(24) Guilmin, P.; Guyot P.; Marchal, G. *Phys. Lett.* **1985**, *109A*, 174.
(25) Clemens, B. M.; Suchoski, M. *J. Appl. Phys. Lett.* **1985**, *47*, 943.
(26) Dufner, D. C.; Eyring, L. *J. Solid State Chem.* **1986**, *62*, 112.
(27) Schwarz, R. B.; Wong, K. L.; Johnson, W. L. *J. Non-Cryst. Solids* **1984**, *61*, *62*, 129.
(28) Meng, W. J.; Nieh, C. W.; Johnson, W. L. *Phys. Rev. Lett.* **1987**, *51*, 1693–1695.
(29) Desre, P. J.; Yavari, A. R. *Phys. Rev. Lett.* **1990**, *64*, 1533–1536.
(30) Johnson, W. L. *Prog. Mater. Sci.* **1986**, *30*, 80–134.
(31) Cotts, E. J.; Meng, W. J.; Johnson, W. L. *Phys. Rev. Lett.* **1986**, *57*, 2295–2298.
(32) Workman, T. W.; Cheng, Y. T.; Johnson, W. L.; Nicolet, M. A. *Appl. Phys. Lett.* **1987**, *50*, 1485–1487.
(33) Cotts, E. J.; Wong, G. C.; Johnson, W. L. *Phys. Rev.* **1988**, *B37*, 9049–9052.
(34) Fister, L; Li, X. M.; McConnel, J; Novet, T.; Johnson, D. C. *Rev. Sci. Instrum.*, submitted for publication.
(35) Novet, T.; Johnson, D. C. *Rev. Sci. Instrum.*, to be submitted for publication.

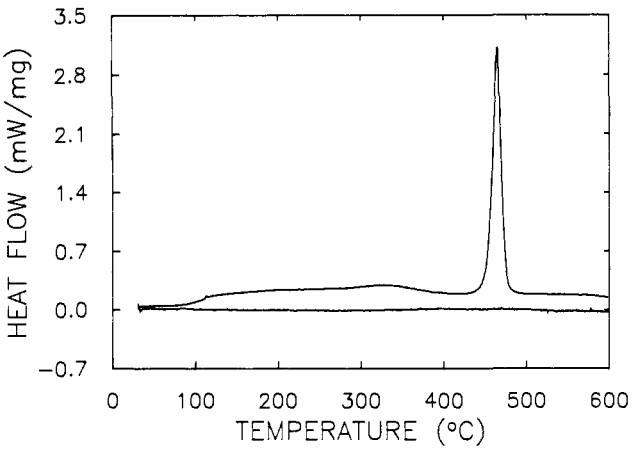

Figure 6. Heat flow rate as a function of temperature obtained for a layered composite of relative composition 1/2 iron/silicon. The upper curve was obtained by heating the sample at 10 °C/min and subtracting a subsequent run on the same sample obtained under identical conditions. The base line is the difference between the heat-flow rates of the second and third heating of the same sample.

multilayer film off of the substrate. Typically, the films broke up and rolled into many small pieces, which were collected via sedimentation into an aluminum DSC pan. The sample was dried under reduced pressure to remove residual acetone. Finally the pan was crimped closed.

The sample was then placed in a Du Pont TA9000 DSC module with an empty pan as the reference container. The sample was heated at 10 °C/min from room temperature to 600 °C under flowing nitrogen. After it was cooled to room temperature, the sample was reheated to obtain a base line for the irreversible changes that occur during the initial heating. A second such background was collected to obtain a measure of the repeatability of the experiment. The net heat absorbed or released from the multilayer sample as it diffuses was obtained from the difference between the first DSC experiment and the subsequent runs. The two background runs were found to be within 0.05 mW/mg of one another.

Results and Discussion

Characterization of the Layered Reactants. The five modulated iron–silicon composites prepared for this study were initially characterized via X-ray diffraction. In all of these samples, there were no diffraction features at high angles, indicating that the layers are amorphous with respect to X-ray diffraction. The modulated electron density in the composites results in a one-dimensional "crystal", which is clearly observed in the grazing-angle diffraction patterns. Figure 5 contains the grazing-angle diffraction pattern of a 10-layer sample of stoichiometry 3/1 iron/silicon with a multilayer spacing of 66 Å.

Qualitatively, the observation of well-resolved beats (the small maxima between the main Bragg diffraction peaks caused by the finite number of unit cells) in the diffraction pattern indicates that the interfacial diffusion region between the iron and silicon layers is planar. It also confirms that the thickness of the iron and silicon layers, the degree of initial diffusion at the interfaces, and the total thickness of the repeat unit is uniform to within 1.5 Å from layer to layer.[36] The ability to observe six Bragg diffraction orders also supports the conclusion that the layer thicknesses are consistent within the multilayer[37] (the sixth diffraction order is visible upon expanding the scale of Figure 5). The intensity of the Bragg peaks, however, drops much more rapidly with diffraction order than would be expected if the sample contained abrupt atomic interfaces between the silicon and iron. The diffraction data suggests that the interface region contains a smoothly varying composition gradient from silicon to iron, which is approximately 20 Å wide.[36] The diffraction patterns obtained for samples prepared with more layers (40–90 layers) typically have only a first- and second-order diffraction peak. We believe that this is a result of increased variation in the deposition rates

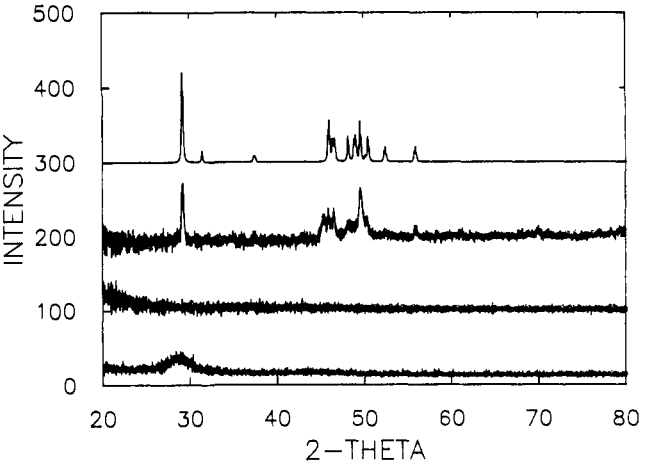

Figure 7. X-ray intensity as a function of 2θ for an as-deposited layered composite of stoichiometry 1/2 iron/silicon (lowest curve), the same sample heated to 300 °C and cooled (second curve from bottom), and the same sample heated to 600 °C and cooled (third curve from bottom). The upper curve is data obtained from the JCPDS diffraction files for a sample of crystalline $FeSi_2$. The curves are offset for clarity.

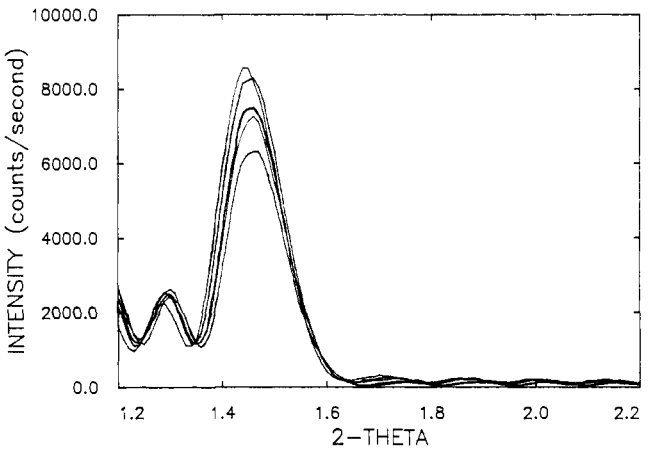

Figure 8. X-ray intensity as a function of 2θ for a layered composite of stoichiometry 3/1 iron/silicon. The upper curve is the initial scan. The lower curves were taken at 1-h intervals while the sample was annealed at 150 °C.

as the deposition sources are depleted, as well as decreased coherence of the entire sample due to an occasional deviant layer.

Reaction Pathway. The irreversible solid-state reactions occurring in the multilayer composites as temperature is raised were studied with differential scanning calorimetry and X-ray diffraction. Figure 6 contains the DSC data for a sample of relative composition 1/2 iron/silicon, which is representative of the data collected from all of the samples. This DSC data has a broad exotherm with an onset temperature of 80 °C, continuing up to the sharp exotherm at 460 °C. Diffraction data collected on a sample heated to 300 °C and subsequently cooled indicated that the sample was no longer layered and that no crystalline phase had formed (Figure 7). Thus, the broad exotherm is caused by interdiffusion of the iron and silicon.[38] Diffraction data collected after heating past the 460 °C sharp exotherm identifies the sample as crystalline $FeSi_2$ (Figure 7).

Temperature-dependent diffraction studies confirm that the broad, low-temperature exotherm in the DSC runs are due to diffusion. The intensity of the low-angle diffraction peaks remains constant as temperature is raised to 80 °C. Above this temperature, the diffraction peaks decrease in intensity as a function of time (Figure 8). At temperatures up to 300 °C, diffraction peaks can still be observed between 1° and 5° (2θ) if high X-ray beam

(36) Nevot, L.; Pardo, B.; Corno, J. *Rev. Phys. Appl.* **1988**, *23*, 1675–1686.
(37) Le Boite, M. G.; Traverse, A.; Nevot, L.; Pardo, B.; Corno, J. *J. Mater. Res.* **1988**, *3*, 1089–1096.

(38) This is confirmed by X-ray diffraction experiments in the temperature range 25-340 °C, vide infra (Figure 7).

Table I. Summary of Thermodynamic Data from Iron–Silicon Multilayers

Fe/Si ratio	diffusion-onset temp (°C)	obsd ΔH_{mixing}[a] (kJ/mol·atom)	obsd $\Delta H_{crystallization}$[a] (kJ/mol·atom)	obsd ΔH_{total}[a] (kJ/mol·atom)	lit. value $\Delta H_{formation}$ (kJ/mol·atom)	crystallization-onset temp (°C)
1/2	80	−20 (4)	−8 (1)	28 (4)	30.6[b]	485
1/1	80	−22 (4)	−4 (0.5)	26 (4)	39.3[c]	290
5/3	80	−30 (4)	−1 (0.3)	31 (4)		455
2/1	80	−37 (4)		37 (4)		
3/1	80	−15 (4)	−1 (0.3)	16 (4)	25.8[d]	540

[a] Values in parentheses are the estimated error bars in the measurement due to the change in the heat capacity of the sample upon crystallization. [b] Reference 44. [c] Reference 45. [d] Reference 46.

intensities are used. After 13 h of heating the sample of 340 °C, no diffraction peaks are observed in the angular range 1–80° (2θ), indicating that the sample is homogeneous and amorphous with respect to X-ray diffraction. The DSC experiments combined with the temperature-dependent X-ray diffraction studies *clearly indicate that we have been able to separate the mixing of the elements from the crystallization of a binary phase. The rate-limiting step in the formation of a crystalline phase from the amorphous alloy is nucleation, not diffusion.*

Interdiffusion and Mixing of Iron and Silicon. The major features of the DSC data are summarized in Table I for all of the samples studied. The data break into two sets, data independent and data dependent upon the composition of the multilayer. The onset of diffusion is found to be independent of composition. The diffusion onset is a measure of the activation energy for diffusion and is dependent upon the structure of the iron–silicon interface. The structure of the interface is a function of deposition conditions and should not be influenced by the overall stoichiometry of the film. Since deposition conditions were constant from sample to sample, the interface structure and therefore the diffusion onset should be composition-independent, as observed.

The heat evolved in the formation of the amorphous alloy from the layered starting reactant is related to ΔH_{mixing}. The exotherms due to mixing are similar to that shown in Figure 6 for all of the samples investigated. The exact shape and magnitude of this exotherm is a function of the layer thicknesses in the initial composite. The absolute errors for the experimental ΔH_{mixing} values are large due to the change in heat capacities of the samples as they go from a layered starting composite to an amorphous alloy to a crystalline compound. These factors tend to increase the measured value of ΔH_{mixing}. An additional error is caused by the broad interface between the iron and silicon due to interdiffusion during deposition. This systematic error will result in a low experimental value for ΔH_{mixing} and depends upon the individual iron and silicon layer thicknesses of each sample.

The heat evolved in the formation of an amorphous alloy from a modulated composite (ΔH_{mixing}) depends upon composition. This evolved heat is a result of the formation of iron–silicon bonds and therefore depends upon the strength as well as the number of bonds in the amorphous alloy. The total number of iron–silicon bonds will be a minimum for compositions that are farthest from equimolar concentration. The smallest ΔH_{mixing} was found for samples with an iron/silicon ratios of 1 to 2 and 3 to 1, respectively. Experimentally, ΔH_{mixing} is larger for compositions closer to an equimolar ratio.

Composition-Directed Crystallization. In addition to the broad low-temp. diffusion exotherm, all of the samples except the eutectic composition show a sharp exotherm. Before this exotherm, the samples are amorphous as determined by X-ray diffraction. Diffraction data collected after these exotherms clearly indicate that the crystalline phase closest in composition to the amorphous alloy was the phase that crystallized. Table II contains the high-angle diffraction data and compares it with that previously reported for crystalline iron silicides.[39–42] Excellent agreement is found between the observed and previously reported peak positions.

Table II. Crystallographic Data for the Iron Silicides

compd	obsd *d* spacing	obsd intens	calcd *d* spacing	calcd intens
$FeSi_2$	3.061	100	3.070	100
	3.051	100	3.060	100
			2.851	20
			2.412	10
			2.400	10
	1.998	43	1.980	50
	1.976	42	1.975	50
	1.956	34	1.960	40
	1.876	46	1.950	40
			1.892	50
			1.867	40
			1.860	40
	1.839	68	1.842	80
	1.817	5	1.822	10
	1.812	19	1.811	50
	1.748	16	1.751	20
	1.741	14	1.746	20
	1.643	20		
FeSi	3.164	8	3.173	22
	2.586	9	2.590	13
	2.236	8	2.243	8
	2.006	100	2.007	100
	1.831	34	1.832	48
			1.587	1
	1.494	2	1.495	3
			1.419	3
	1.352	7	1.353	8
	1.293	2	1.295	3
	1.242	3	1.244	4
	1.199	13	1.199	20
Fe_5Si_3			3.350	10
			2.920	10
			2.740	10
			2.350	20
			2.210	60
	2.001	100	2.000	100
			1.940	80
			1.920	80
	1.832	12	1.830	10
			1.375	80
			1.620	10
			1.590	40
			1.530	10
			1.460	30
			1.375	50
			1.330	20
			1.291	10
	1.277	9	1.282	80
			1.244	50
Fe_3Si	3.274	1	3.250	40
	2.832	1	2.830	40
	2.007	100	1.990	100
	1.711	3	1.700	40
			1.620	20
	1.418	15	1.410	100
	1.277	3		

The heats of crystallization of the binary silicides from the amorphous alloys are summarized in Table I. The heats of crystallization ($\Delta H_{crystallization}$) reflect the differences in structure (bond lengths and angles) between the amorphous and crystalline

(39) Bucksch, Z. *Z. Naturforsch.*, A: *Phys. Sci.* **1967**, *22*, 2124.
(40) Wong-Ng, W.; McMurdie, H.; Poretzkin, B.; Hubbard, C.; Drago, A. *Powder Diffr.* **1987**, *2*, 261.
(41) Yu, Z. *Acta Petrol. Mineral. Anal.* **1984**, *3*, 23.
(42) Keil, K. *Am. Mineral.* **1982**, *67*, 126.

states. The largest heat of crystallization was found for the most silicon-rich iron silicide, $FeSi_2$, which is a semiconductor and only forms in a narrow composition range. The more iron-rich binary silicides are metallic and have structures consistent with metallic bonding.[43] They evolve less heat upon crystallization, which can be rationalized as a result of the less directional nature of metallic bonding. The small heat of crystallization of Fe_3Si reflects the large amount of disorder in the structure as inferred by its stability over a broad range of composition. The small heat of crystallization observed for Fe_5Si_3 may result from its metastability at the temperature at which it nucleates.

Heats of Formation. The total heat evolved in the formation of each phase is the sum of the energy of mixing and the energy during crystallization. An important point our data illustrates is that the majority of the heat of formation of a crystalline compound is a result of the mixing of the elements. The actual ordering of the amorphous alloy to form the crystalline compound produces only a small fraction of the heat of formation of the crystalline compound. The large energy of mixing is due to the formation of iron–silicon bonds. Crystallization optimizes the bonding already existing in the amorphous alloy.

The total heat evolved during the heat treatment of these films is compared with published values for the heats of formation of the crystalline compounds determined via other techniques in Table I.[44-46] Our values are consistently less than these published values as a result of the mixing that occurs during deposition. The broad interface formed during deposition results in a low experimental value for the ΔH_{mixing}.

Nucleation Temperatures. Table I also contains the crystallization temperature of the different compounds from their respective amorphous films. FeSi, the expected first phase to form from the first-phase rule,[17] has the lowest crystallization temperature. It is the easiest binary silicide to nucleate from an amorphous alloy. Previous literature reports have stated that FeSi nucleates at temperatures between 240 and 400 °C.[47,48] Crystallization temperatures are very sensitive to impurities as well as to the nature of the substrate. We have qualitatively observed that the crystallization of the films depends upon exposure to oxygen. Amorphous films annealed at 300 °C in an inert atmosphere will crystallize within 5 min after exposure to atmospheric oxygen at room temperature.

Crystallization of iron silicides from an amorphous composite clearly depends upon the composition of the amorphous alloy. To further explore the effect of composition upon nucleation, we prepared an amorphous alloy containing 34 atomic percent iron. This composition corresponds to a eutectic, with Fe_3Si and Fe_5Si_3 the closest crystalline phases in composition. The DSC data up to 600 °C for this sample did not contain any exothermic signals expected if the sample crystallized. The X-ray diffraction results confirmed that the sample was still amorphous after heating to 600 °C. Further studies into the composition dependence of nucleation of a crystalline phase from amorphous alloys are being conducted.

Nucleation of Metastable Compounds. The use herein of ultrathin-film modulated composites represents a unique, controlled approach to the synthesis of metastable compounds. The concept demonstrated in this paper is that the rate-limiting step in the formation of a crystalline phase in this low-temperature synthesis method is nucleation. *Metastable phases will form if they are easier to nucleate than the more thermodynamically stable phases.* An example of this phenomenon is found in this study of the Fe–Si system, where we observed the crystallization of an amorphous alloy with an iron/silicon ratio of 5 to 3 to the crystalline phase Fe_5Si_3 at a temperature of 500 °C. From the bulk phase diagram (Figure 4), Fe_5Si_3 is thermodynamically unstable with respect to a mixture of Fe_3Si and FeSi at temperatures below 825 °C.

Summary

Our synthetic approach is summarized in Figure 1. This is a unique controlled reaction pathway for a solid-state reaction, which enables one to separate the energies associated with the intermixing of the elements from the crystallization energy of a particular compound. In this paper, we have shown the following:

(1) A controlled synthetic approach to the formation of extended crystalline solids in which thin (~30 Å), amorphous elemental layers are sequentially deposited creates a uniquely characterizable solid-state reactant. The modulated structure of this reactant can be engineered to vary composition and diffusion distances.

(2) Diffusion in the modulated composite can be initiated at low temperatures ($80 < T < 400$ °C) to produce a homogeneous amorphous alloy, a novel synthetic intermediate.

(3) The thereby designed rate-limiting step in the formation of a crystalline material is nucleation.

(4) The composition of the amorphous alloy can be used both to direct and to control the nucleation of crystalline iron silicides.

The ability to form metastable materials from amorphous alloys should permit the extension of the concepts herein to rationally synthesize many ternary compounds that are unstable with respect to binary compounds. Such ternary compounds are inaccessible via traditional synthetic methods, and, in fact, it is such ternary compounds that are one of our major goals. Research in this direction is currently under investigation.

Acknowledgment. We are pleased to acknowledge the assistance of L. Fister, J. McConnell, and C. Grant in developing the experimental procedures used in this paper. This work was supported by a Young Investigator Award from the Office of Naval Research (No. N00014-87-K-0543). Grants by the National Science Foundation (DMR-8704652), the donors of the Petroleum Research Fund, administered by the American Chemical Society, and a starter grant from the University of Oregon are also gratefully acknowledged.

Registry No. Fe, 7439-89-6; Si, 7440-21-3; $FeSi_2$ (alloy entry), 37237-02-8; $FeSi_2$ (inorganic entry), 12022-99-0; FeSi (alloy entry), 11135-64-1; FeSi (inorganic entry), 12022-95-6; Fe_5Si_3 (alloy entry), 132645-89-7; Fe_5Si_3 (inorganic entry), 12023-77-7; Fe_2Si (alloy entry), 12664-14-1; Re_2Si (inorganic entry), 11148-61-1; Fe_3Si (inorganic entry), 12023-54-0.

(43) Wells, A. F. *Structural Inorganic Chemistry*; Clarendon Press: Oxford, 1984; pp 987, 1290–1300.
(44) Gorelkin, O. S.; Mikhailov, S. V. *Russ. J. Phys. Chem.* (*Engl. Transl.*) **1971**, *45*, 1523; *Zh. Fiz. Khim.* **1971**, *45*, 2682.
(45) Jounel, B.; Mathieu, J. C.; Desre, P. *C. R. Acad. Sci., Ser. 3* **1968**, *266*, 773.
(46) Sommer. F. *J. Therm. Anal.* **1988**, *33*, 15.
(47) Oswald, R. S.; Ron, M.; Ohring, M. *Solid State Commun.* **1978**, *26*, 883–887.
(48) Cheng, H. C.; Yew, T. R.; Chen, L. J. *J. Appl. Phys.* **1985**, *57*, 5246–5250.